Published OnlineFirst March 29, 2016; DOI: 10.1158/0008-5472.CAN-15-2347

Molecular and Cellular Pathobiology

Cancer Research

A CDK4/6-Dependent Epigenetic Mechanism Protects Cancer Cells from PML-induced Senescence

Mariana Acevedo, Mathieu Vernier, Lian Mignacca, Frédéric Lessard, Geneviève Huot, Olga Moiseeva, Véronique Bourdeau, and Gerardo Ferbeyre

Abstract

Promyelocytic leukemia (PML) plays a tumor suppressive role by inducing cellular senescence in response to oncogenic stress. However, tumor cell lines fail to engage in complete senescence upon PML activation. In this study, we investigated the mechanisms underlying resistance to PML-induced senescence. Here, we report that activation of the cyclin-dependent kinases CDK4 and CDK6 are essential and sufficient to impair senescence induced by PML expression. Disrupting CDK function by RNA interference or pharmacological inhibition restored senescence in tumor cells and diminished their tumorigenic potential in mouse xenograft models. Complete senescence correlated with an increase in autophagy, repression of E2F target genes, and an gene expression signature of blocked DNA methylation. Accordingly, treatment of tumor cells with inhibitors of DNA methylation reversed resistance to PML-induced senescence. Further, CDK inhibition with palbociclib promoted autophagy-dependent degradation of the DNA methyltransferase DNMT1. Lastly, we found that CDK4 interacted with and phosphorylated DNMT1 *in vitro*, suggesting that CDK activity is required for its stabilization. Taken together, our findings highlight a potentially valuable feature of CDK4/6 inhibitors as epigenetic modulators to facilitate activation of senescence programs in tumor cells. *Cancer Res; 76(11); 3252–64. ©2016 AACR.*

Introduction

PML was originally identified as the target of chromosome translocations in acute promyelocytic leukemia (APL; ref. 1) and as an important regulator of cellular senescence in response to oncogenes or short telomeres (2–4). PML-induced senescence underlies the success of the treatment of APL with retinoic acid (5). PML forms characteristic nuclear bodies that have been associated to its tumor suppressor functions enhancing the activities of the tumor suppressors p53 and RB and repressing the functions of the oncogenic kinase Akt (2, 6). The ability of PML to induce senescence in primary human cells hinges on the RB-dependent suppression of E2F-target genes expression (2, 7–9).

Senescence acts as a tumor suppression mechanism early during carcinogenesis by imposing a proliferation barrier to cells expressing oncogenic mutations. In addition, senescence cells activate immune-mediated mechanisms that result in their clearance (10). The senescence process induced by oncogenes in primary cells can be bypassed by mutations that inactivate the tumor suppressors p53, RB, or PML (10). However, tumor cells can enter senescence after conventional chemotherapy, indicating that the program is not fully disabled (11). Although chemotherapy-induced senescence in cancer cells share some biomarkers with the senescence response of primary cells, it is not yet clear whether its outcome is equally effective. In particular, it is still unknown how the multiple genetic and epigenetic changes present in tumor cells affect the efficacy of the senescence program in terms of the stability of the cell-cycle arrest and the recruitment of an effective antitumor immune response.

Our current ability to study tumor cell senescence is limited by the still poor understanding of the senescence process and the lack of definitive, reliable biomarkers. The senescence-associated β-galactosidase (SA-β-Gal), the most used senescence marker, is in fact a lysosomal enzyme (12) whose activity is increased due to a general activation of autophagy in senescent cells (13, 14). In immortalized cells, oncogenic *ras* can induce several senescence biomarkers without causing a complete growth arrest. This process, called senescence with incomplete growth arrest or SWING (15), suggests that there is more than one phenotype associated to what we call today cellular senescence. The phenomenon of senescent cell clearance *in vivo* may circumvent the requirement for a tight growth arrest to achieve tumor suppression. However, senescent cells in benign tumors can persist for years without progression to malignant lesions (16), indicating that blocking cell-cycle progression is an important part of the senescent tumor suppression mechanism. Several studies indicate that the tumor suppressors RB and PML control the reversibility of the senescence program by regulating the repression of E2F target genes (8, 17–19). In some cell types, this process involves the formation of heterochromatin structures known as senescence-associated heterochromatin foci or SAHF (20). SAHF require high mobility group A (HMGA) proteins (21) and histone-modifying enzymes that catalyze the introduction of heterochromatin marks (22). However, SAHF are not universal biomarkers of senescence and the heterochromatin

Department of Biochemistry and Molecular Medicine, Université de Montréal, Montréal, Québec, Canada.

Note: Supplementary data for this article are available at Cancer Research Online (http://cancerres.aacrjournals.org/).

Corresponding Authors: Véronique Bourdeau, University of Montreal, C.P. 6128, Succ. Centre-Ville, Montreal, Quebec H3C3J7, Canada. Phone: 514-343-7571; Fax: 514-343-2210; E-mail: veronique.bourdeau@umontreal.ca; and Gerardo Ferbeyre, g.ferbeyre@umontreal.ca

doi: 10.1158/0008-5472.CAN-15-2347

modifications associated with them may also play a role protecting tumor cells from DNA damage signaling (23). It is thus clear that other regulatory layers remain to be identified to understand gene expression control in senescent cells.

Here, we investigate the mechanism of resistance of tumor cells to PML-induced senescence. We first found that expression of CDK4 and CDK6 kinases inhibited PML-induced senescence in normal cells. In tumor cells, where these kinases are deregulated, PML induced an incomplete senescence program, which was restored by knockdown of CDK4 and CDK6 or expression of the CDK inhibitors p21 or p16INK4a. The CDK inhibitors flavopiridol or palbociclib (PD0332991) also increased the ability of PML to regulate tumor cell senescence in culture and reduced tumor progression *in vivo*. Transcriptome analysis of cells expressing PML and treated with palbociclib showed that senescence correlated with a better repression of E2F target genes and unexpectedly with a gene expression signature previously described in cells exposed to a DNA methylation inhibitor. Inhibition of DNA methylation restored the full senescence response to PML in tumor cells. CDK inhibitors acted on this pathway by promoting the autophagy-dependent degradation of DNMT1. Conversely CDK4/6 interact with and phosphorylate DNMT1 increasing its stability. Together, the results indicate that CDK4/6 kinases maintain an epigenetic mechanism that protect tumor cells from senescence and provide a proof of concept for a senescence therapy of cancer using CDK4/6 inhibitors.

Materials and Methods

Cells, retroviral gene transfer, plasmids, and reagents

PC3, U2OS, HEK-293T, and normal human diploid fibroblasts IMR90 cells were obtained from ATCC. Phoenix ampho packaging cells were a gift from (S.W. Lowe, Memorial Sloan Kettering Cancer Center, New York, NY). PC3 cells were cultured in RPMI medium (Wisent) supplemented with 10% FBS (Wisent), 1% penicillin/streptomycin sulfate (Wisent), and 2 mmol/L L-glutamine (Wisent). All other cell lines were culture in DMEM (Wisent) supplemented with 10% FBS and 1% penicillin/streptomycin sulfate. Retroviral-mediated gene transfer, growth curves, and SA-β-Gal activity were assayed as described in ref. 2.

Retroviruses pLPC, pLPC-PML, pWZL, and pWZL-PML (isoform IV) were described in ref. 2. pBABE-CDK4 and pBABE-CDK6 were a gift from S.W. Lowe. Retroviral vectors for WZL-CDK4 wild-type and K35M mutant were a gift from G.J. Hannon (Cold Spring Harbor Laboratory, Cold Spring Harbor, NY). Flag variants for CDK overexpression of CDK2(WT), CDK4(WT), and mutant K35M were PCR amplified with a primer containing the 3xFLAG tag and subcloned in *Bam*HI/*Eco*RI restriction sites to create pBABE-3xFLAG-CDK2(WT), pBABE-3xFLAG-CDK4(WT), and pBABE-3xFLAG-CDK4mut(K35M). Retrovirus pLPC-3xFLAG was described in ref. 8. pcDNA3-Myc-DNMT1 was purchased from Addgene. Retroviral vectors with shRNAs against RB or the RB pocket proteins were also obtained from S.W. Lowe and described in ref. 18. CDK4 and/or 6 shRNAs were cloned in retroviral vectors pMLP (MSCV-based vector expressing shRNA in a miR30 context) or pMLPX (24). shRNA mature sequences are mentioned in Supplementary Material. pBABE-ER vector was a gift from S.W. Lowe and PML (isoform IV) was obtained by PCR from pLPC-PML (2) and subcloned between *Bam*HI/*Xho*I restriction sites to create pBABE-PML_{IV}-ER.

The CDK inhibitor flavopiridol was purchased from Selleckchem. Palbociclib (PD0332991), 5-Aza-2′-deoxycytidine (5-Aza-dC), OHT (4-hydroxytamoxifen), and bafilomycin A1 were purchased from Sigma-Aldrich. Treatments at the indicated concentrations with flavopiridol, palbociclib, and OHT were renewed every 3 days and 5-Aza-dC was added once for three days.

Immunoblotting and immunofluorescence

Protein expression analysis was performed as described in ref. 8. Antibodies, immunoprecipitation protocol, and *in vitro* protein kinase assays are described in Supplementary Materials and Methods. For immunofluorescence studies, cultured cells were plated on coverslips and fixed as described in ref. 8. For LC3B and p62 immunodetection, cells were treated 24 hours with bafilomycin A1 (50 nmol/L) prior to fixation. The primary antibodies used were: anti-53BP1 rabbit polyclonal (1:200, EMD Millipore #PC712), anti-DNMT1 rabbit polyclonal (1:200, Cell Signaling Technology, #5032), anti-PML mouse monoclonal (1:400, Santa Cruz Biotechnology PG-M3), anti-LC3B rabbit polyclonal (1:400, Cell Signaling Technology, #2775), or anti-SQSTM1/p62 rabbit polyclonal (1:400, Cell Signaling Technology, #5114). Secondary antibody combinations used were: Alexa-Fluor 488 goat anti-mouse and Alexa-Fluor 568 goat anti-rabbit (1/2000, Molecular Probes, Invitrogen). We used as mounting media ProLong Gold Antifade Reagent with DAPI (Invitrogen). Images were collected on an upright microscope Axio Imager.Z2 (Zeiss) with the Zen Microscope and imaging software.

Animals

Mouse experiments were conducted in accordance with institutional and national guidelines and regulations. For xenografts, 30 BALB/c 6-week-old nude mice (Charles River) were injected subcutaneously in both flanks with 10^6 PC3 cells expressing empty vector (V) or PML. Cells were suspended in PBS mixed with Matrigel (BD Biosciences). Tumor formation was followed every 2 days for a period of 18 days. When tumors reached around 150 mm^3, mice were separated in three treatment groups for each condition: NT, nontreated (control); Fl, flavopiridol (5 mg/kg/day diluted in 0.9% NaCl-0.1% DMSO injected intraperitoneally); Pa, palbociclib (PD 0332991: 100 mg/kg/day diluted in sodium lactate 50 mmol/L pH 4 administered by gavage).

Mice were treated for 5 consecutive days. Tumor growth was measured every 2 days for the following 22 days without further treatments. Statistical analysis was performed using SPSS software 16.0 (SPSS, Inc.). The nonparametric Kruskal–Wallis test was used to show significant differences in tumor growth among groups. All values were expressed as mean (± SE of the mean; SEM). A P value of less than 0.05 was accepted as statistically significant. Mice were euthanized before the endpoint of the experiment when tumor volume reached 2 cm^3. Tumors were collected and either snap frozen (for later RNA extractions) or fixed in 10% neutral-buffered formalin solution, paraffin embedded, and cut into sections for immunofluorescence analysis.

Immunofluorescence from paraffin-embedded samples

Tumor sections from xenografts were deparaffinized and rehydrated. Antigen epitope retrieval was performed by heating for 25 minutes at 95°C in sodium citrate buffer (10 mmol/L sodium citrate, 0.05% Tween 20, pH 6.0). Samples were permeabilized with Triton 0.5%-PBS 1X solution for 15 minutes and blocked with 3% BSA, 5% goat serum, 0.1% Tween 20-PBS 1X solution for 1 hour. Samples were incubated with the primary antibody at 4°C overnight as follows: anti-PML (mouse monoclonal, PG-M3

Published OnlineFirst March 29, 2016; DOI: 10.1158/0008-5472.CAN-15-2347

SC966; Santa Cruz Biotechnology; 1:400); anti-LC3B (rabbit polyclonal, 2775S; Cell Signaling Technology; 1:400); anti-SQSTM1/p62 (rabbit polyclonal, 5114; Cell Signaling Technology; 1:400). The next day, samples were washed in PBS 1X and incubated with goat anti-mouse AlexaFluor 488 (1:1,000; A-11029, Molecular Probes, Invitrogen) or anti-rabbit AlexaFluor 568 (1:1,000; A-11036, Molecular Probes, Invitrogen). For mounting, we used ProLong Gold Antifade Reagent with DAPI (P36931; Invitrogen).

RNA expression analysis

Snap-frozen tumor samples were transferred to RLT buffer (Qiagen) for homogenization first with micropestels and then by passing the samples through QIAshredder column (Qiagen) prior to RNA isolation with RNeasy Mini Kit (Qiagen) according to the manufacturer's instructions. Cultured cells were collected in TRIzol reagent (Invitrogen) for RNA extractions, according to the manufacturer's instructions and RNA samples sent for gene arrays (Human Gene 2.0 ST Array, at the McGill University and Génome Quebec Innovation Center, Montreal, Quebec, Canada) were further purified with RNeasy MinElute Cleanup Kit (Qiagen).

The microarray data files from triplicates of the four conditions were analyzed with the Affymetrix Expression Console Software and Transcriptome Analysis Console (www.affymetrix.com). Raw data were normalized with a Robust Multi-array Average (RMA) algorithm. The microarray data were deposited in NCBI's Gene Expression Omnibus (GEO) and are accessible through GEO Series accession number GSE70923.

The gene set enrichment analysis (GSEA) software was used to match gene expression patterns in our four conditions with gene sets available in the Molecular Signature Database (MSigDB). The significance of enrichment values (NES) was determined by the false discovery rate (FDR; q value) and by a nominal P value calculated by an empirical phenotype-based permutation test procedure as described previously (25). Only enriched gene sets with a P value ≤ 0.05 and a q value ≤ 0.25 were considered significant. A detailed explanation of our bioinformatic analysis was previously published in ref. 26.

Quantitative real-time PCR was performed as described in ref. 8. Primer sequences are available in Supplementary Material and Methods.

Results

Expression of cyclin-dependent kinases CDK4 and CDK6 suppresses PML-induced senescence

To investigate the mechanisms allowing tumor cells to evade senescence, we first tested whether expression of the kinases CDK4 and CDK6 could prevent PML-induced senescence in normal human fibroblasts. We found that these kinases efficiently blocked PML-induced growth arrest and senescence in normal cells (Fig. 1A and Supplementary Fig. S1A–S1C). One important function of PML during senescence involves RB and the repression of E2F target genes (8). Accordingly, the expression of CDK4 or CDK6 was able to restore the expression of multiple E2F targets in PML-expressing cells (Supplementary Fig. S1D). In a similar way, RB knockdown but not p107 or p130 knockdown suppressed PML-induced senescence and increased the expression of E2F target genes (Supplementary Fig. S1E–S1H). Together, these experiments indicate that expression of CDK4 or CDK6 beyond a certain threshold can overcome the ability of PML to engage the RB pathway and induce senescence in normal cells.

As cancer cells have defects in the RB pathway, we anticipated that PML could induce a better senescence response in tumor cells if the functionality of the RB pathway is strengthened. Thus, to investigate whether CDK inhibition could improve the ability of PML to inhibit the growth of tumor cells, we co-expressed PML with shRNAs against CDK4, CDK6, or a construct expressing shRNAs simultaneously against CDK4 and CDK6. In U2OS cells, PML reduced cell growth but shRNAs against CDK4 or CDK6 did not. Combining shCDK4 and shCDK6 slightly reduced cell growth but in combination with PML expression, we observed a stronger growth reduction (Fig. 1B). In PC3 prostate cancer cells, PML also inhibited cell growth and this effect was enhanced by coexpressing shRNAs against CDK4 or 6 and even more when both shRNAs were coexpressed (Fig. 1C). shCDK4 and shCDK6 efficiently reduced the levels of their targets when used alone or when expressed together in the same vector (Fig. 1D). We also assessed RB levels in U2OS cells expressing PML and the different shRNAs. RB levels in senescent cells appear reduced in Western blots (Fig. 1D; ref. 7). Another hallmark of senescence is the accumulation of DNA damage foci, which we measured with antibodies against the DNA damage response protein p53BP1. Downregulation of CDK4/6 with shRNAs (two different combinations of shRNAs against CDK4 and CDK6) increased the number of U2OS cells with several p53BP1 foci and expression of PML further increased the number of these foci (Fig. 1E). Senescence is also characterized by an increase in autophagy markers (13). The lipid-conjugated form of LC3 known as LC3B accumulates in senescent cells when the autophagy flux is inhibited with vacuole ATPase inhibitors such as bafilomycin A1 (13). We found that cells expressing PML and shRNAs against CDK4/6 accumulate the autophagy markers LC3B and p62 (Fig. 1F). This is best illustrated using single-cell analysis by immunofluorescence using antibodies specific for these markers. The number of cells having high numbers of LC3B and p62 foci is much higher after combining PML with shCDK4/6 (Fig. 1G and H). To confirm our shRNA results, we next inhibited CDKs by forcing the expression of the CKIs p21 and p16INK4A (Supplementary Fig. S2A and S2B). Both p21 and p16INK4A expression inhibited the growth of U2OS (Supplementary Fig. S2C) and PC3 cells (Supplementary Fig. S2D) and cooperated with PML to further inhibit cell growth.

Next, we tested whether pharmacologic inhibitors of CDKs also cooperated with PML to reduce cancer cell proliferation. We used flavopiridol, a drug that inhibits several CDKs (27) and palbociclib (PD0332991), a selective and potent inhibitor of CDK4 and CDK6 (28). In PC3 cells, the combination flavopiridol–PML was slightly better than PML alone to reduce cell growth (Fig. 2A) and induce senescence (Fig. 2C). In contrast, combining palbociclib with PML was dramatically more effective (Fig. 2B and C). The autophagy/senescence markers LC3B and p62 accumulated at higher levels in cells expressing PML and treated with the CDK inhibitors (Fig. 2D–F). Similar results were obtained in U2OS cells (Supplementary Fig. S3). These results are consistent with the idea that CDK inhibitors potentiate the senescence tumor-suppressive functions of PML.

To obtain *in vivo* evidence that CDK inhibitors and PML cooperate in tumor suppression, we prepared PC3 cells expressing PML or a vector control and injected them in the flanks of nude mice. The animals were then divided in six groups each with 5 animals injected in each flank. Three groups have an empty vector and were treated for five consecutive days with vehicle (V/NT), flavopiridol (V/Fl), or palbociclib (V/Pa). The other groups

Published OnlineFirst March 29, 2016; DOI: 10.1158/0008-5472.CAN-15-2347

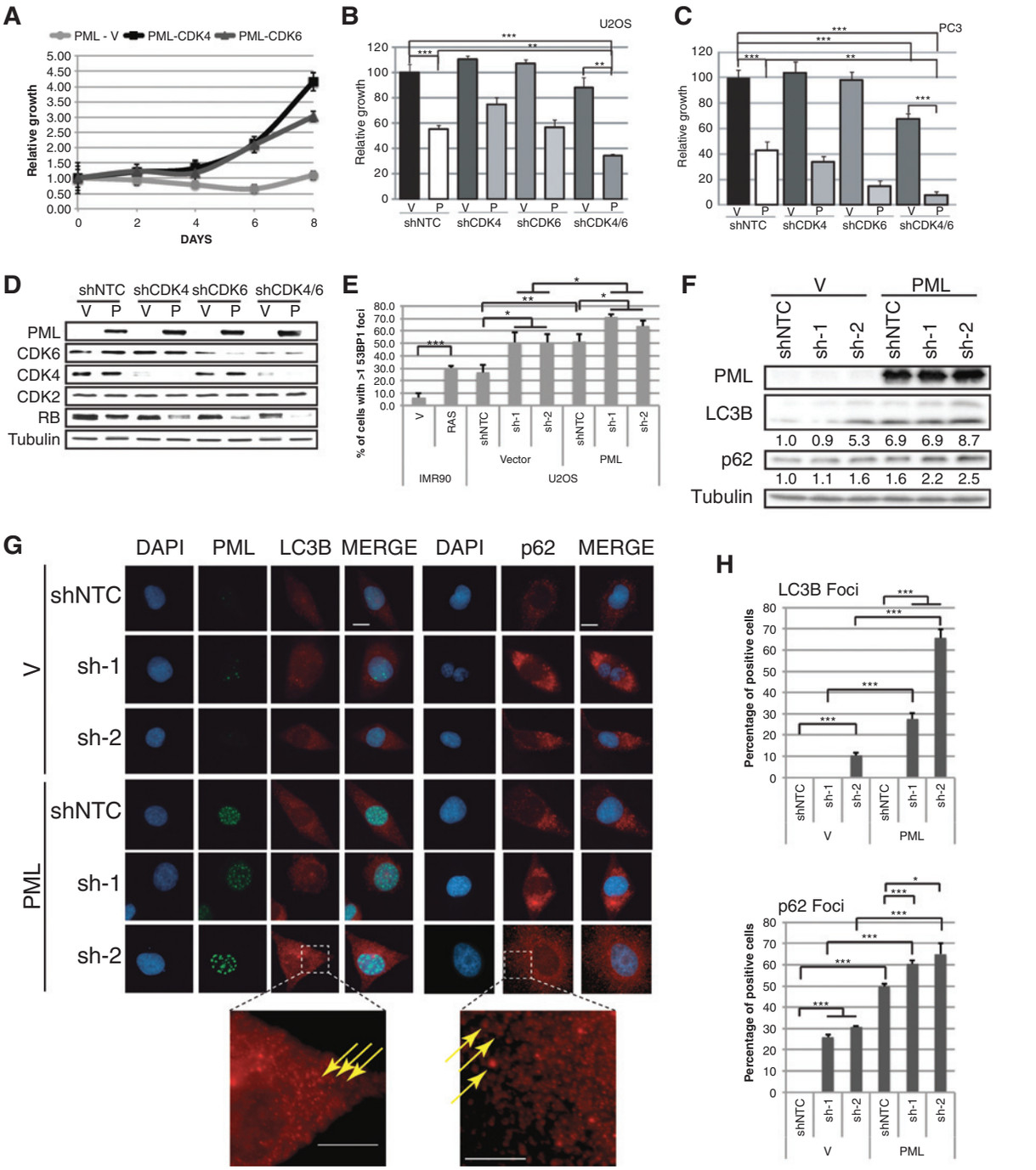

Figure 1.
CDK4/6 kinases suppress PML-induced senescence. A, cell growth estimated from a crystal violet retention assay of IMR90 cells expressing PML together with a vector control (V), CDK4 or CDK6. B, relative growth of U2OS cells infected with empty vector (V) or a vector-expressing PML (P) as well as a vector expressing either a control nontargeting shRNA (shNTC), an shRNA against CDK4 (shCDK4), CDK6 (shCDK6), or two shRNAs targeting CDK4 and CDK6 (shCDK4/6). C, relative growth of PC3 cells modified as in B. D, immunoblots against the indicated proteins using U2OS cells as in B. E, quantification of DNA damage foci per cells after indirect immunofluorescence for 53BP1 in IMR90 cells infected with control vector (normal) or oncogenic Ras (senescent) and in U2OS cells bearing an empty vector (V) or PML and further modified with a control nontargeting shRNA (shNTC), or double shRNAs, shCDK4/6-1 and shCDK4/6-2 (sh1 or sh2). F, immunoblots against the indicated proteins using U2OS cells as in E. G, fluorescent imaging of LC3B and p62 foci as markers of autophagy (red) of U2OS cells as in E and treated with 50 nmol/L bafilomycin A1 for 24 hours. PML staining is shown in green and nuclear DNA (DAPI) in blue. Scale bar, 10 μm. H, quantification of LC3B and p62 foci per cells using data from multiple immunofluorescence images as in G. Cells presenting more than 100 foci were considered positive for induction of autophagy. Three sets of 100 cells were looked at. Error bars, mean ± SD, *, $P < 0.05$; **, $P < 0.01$; and ***, $P < 0.005$ using Student t test.

Published OnlineFirst March 29, 2016; DOI: 10.1158/0008-5472.CAN-15-2347

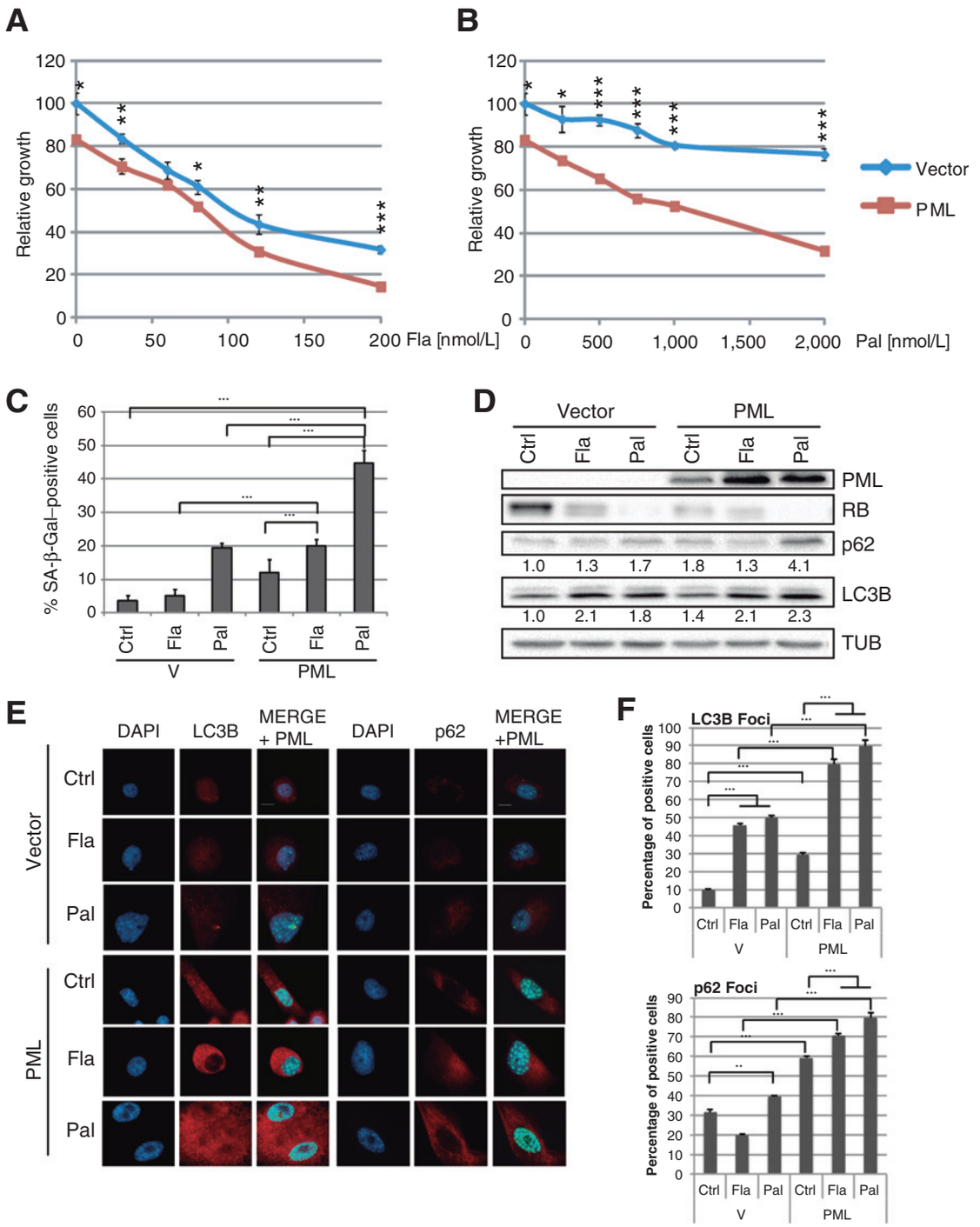

Figure 2.

CDK inhibitors enhance PML-mediated growth arrest and senescence in tumor cell lines. A and B, relative growth of PC3 cells infected with empty vector or a vector-expressing PML treated with flavopiridol (Fla; A) or palbociclib (Pal; B) at the indicated doses for 6 days. Error bars, mean ± SD, *, $P < 0.05$; **, $P < 0.01$; and ***, $P < 0.005$ using Student t test. C, SA-β-Gal in PC3 cells infected with empty vector (V) or a vector-expressing PML treated with vehicle (Ctrl), 120 nmol/L flavopiridol (Fla), or 500 nmol/L palbociclib (Pal). D, immunoblots for the indicated proteins in cells as in C. TUB, tubulin E, LC3B and p62 foci (red) visualized after immunofluorescence staining of PC3 cells as in C. PML staining is shown in green and nuclear DNA (DAPI) in blue. Scale bar, 10 μm. F, quantification of LC3B and p62 foci per cells of immunofluorescence performed in E. Cells presenting more than 100 foci were considered positive for induction of autophagy. Three sets of 100 cells were looked at. Error bars, mean ± SD, *, $P < 0.05$; **, $P < 0.01$; and ***, $P < 0.005$ using Student t test.

Published OnlineFirst March 29, 2016; DOI: 10.1158/0008-5472.CAN-15-2347

expressed PML and were also treated for five days with vehicle (PML/NT), flavopiridol (PML/Fl), or palbociclib (PML/Pa). Tumors with an empty vector or PML progressed without treatment, although PML moderately reduced tumor growth. Treatment with CDK inhibitors reduced tumor growth but the best results were obtained in PML-expressing tumors after treatment with either flavopiridol or palbociclib (Fig. 3A–C). In fact, the combination of PML and CDK inhibitors completely eliminated the tumors in some animals, suggesting either tumor cell death or clearance by the innate immune system. Of note, all tumors recovered from PC3-PML had a reduction in the expression level of retroviral transcripts (Fig. 3D), suggesting a preferential growth *in vivo* of cells with less transcription of the expression vector and explaining why in some animals the treatment did not totally eliminate the tumors. As shown previously with cells in culture, the combination of PML with CDK inhibitors induced a higher accumulation of the autophagy markers LC3B and p62 when analyzed several days after the treatment was stopped (Fig. 3E and F).

Gene expression profile of cells expressing PML and treated with CDK inhibitors

We next compared the transcriptome of PC3 cells expressing PML or a vector control and treated with palbociclib or vehicle. The comparisons of control cells with cells expressing PML or treated with palbociclib are described in the Supplementary Fig. S4. In general, both PML and palbociclib regulate cell cycle, E2F targets, and interferon genes although obviously these changes were not sufficient to trigger a stable senescence response. Next, we compared senescent cells (PML-expressing and palbociclib-treated PC3 cells), with either PC3 cells expressing a vector control treated with palbociclib or PC3 cells expressing PML but not treated with palbociclib (Supplementary Fig. S5). These evaluations are expected to reveal the critical gene expression changes associated to stable senescence, especially those that are common to both comparisons. One hallmark of senescence is the upregulation of genes involved in inflammation and the immune response (29). Consistent with the senescence phenotype induced by the combination of PML and palbociclib, several cytokine genes were found upregulated in this condition in comparison with cells expressing PML alone or cells treated with palbociclib (Supplementary Fig. S5A and S5B). Another characteristic of senescent cells is the downregulation of E2F target genes (8, 18). As mentioned above, both PML and palbociclib when used alone induced a downregulation of several E2F targets in PC3 cells (Supplementary Fig. S4D and S4H) but their combination was even more effective, increasing the number of E2F targets that are downregulated (Supplementary Fig. S5C and S5D). Intriguingly, we found a downregulation of several E2F target genes that play a role in DNA repair in cells treated with PML and palbociclib (Supplementary Fig. S5E and S5F). This is consistent with previous findings during PML-induced senescence in primary fibroblasts (8), suggesting a mechanism to explain the persistent DNA damage response seen in senescent cells.

Remarkably, the gene expression pattern of PML/palbociclib-treated cells overlaps with the pattern observed in pancreatic cancer cells treated with DNA methylation inhibitors (Fig. 4A and B). *CDC2*, *CDC6*, *CENPF*, *FOXM1*, *LMNB1*, and *HMGB2*, were among the genes downregulated in cells treated with DNA methylation inhibitors (30). We confirmed their enhanced downregulation in PML/palbociclib-treated cells when compared with control growing cells expressing empty vectors, control cells treated with palbociclib, or cells expressing PML alone (Fig. 4C). In addition, we confirmed that PML/palbociclib treatment increased the levels of several senescence-regulatory genes repressed by DNA methylation. They include EDN1 (31), GADD45A (32), IFI44L (33), IL23A (34), and SerpinE1/PAI1 (Fig. 4D; ref. 5). Together, the gene expression pattern suggests that the prosenescence interaction between PML and palbociclib involves the control of DNA methylation.

DNA methylation and DNMT1 control tumor cells resistance to senescence

To investigate whether gene regulation due to DNA methylation plays a role in the resistance of tumor cells to PML-induced senescence, we treated PC3 prostate cancer cells with the DNA methyl transferase inhibitor 5-aza-2′deoxycytidine (5-Aza-dC). The drug decreased cell growth in control cells but the effect was more pronounced when combined with PML expression (Fig. 5A). Hence, DNA methylation inhibitors, like CDK inhibitors, cooperate with PML to induce growth arrest. Next we investigated whether 5-Aza-dC cooperated with PML to induce senescence. Treatment of PC3 cells with 5-Aza-dC at doses between 40 and 250 nmol/L only slightly induced SA-β-Gal activity, similar to PML expression alone. However, combining PML expression with the drug induced a dose-dependent SA-β-Gal activity in these cells (Fig. 5B). Similar results were found when using autophagy markers LC3B and p62, which were both more abundant in cells treated with 5-Aza-dC and expressing PML (Fig. 5C and D).

To further confirm that PML and 5-Aza-dC cooperate to induce senescence we prepared PC3 cells expressing a PML fusion protein with the ligand binding domain of the estrogen receptor (PML-ER) that is active in the presence of OHT. In normal fibroblasts expressing PML-ER, treatment with OHT for one week induced a senescent cell-cycle arrest where 96% of the cells were positive for SA-β-Gal (Supplementary Fig. S6A). To study the reversibility of this phenotype, we treated PML-ER–expressing normal fibroblasts for 1, 2, 3, 4, and 7 days with OHT and then cultured them for another 5 days without OHT. We found that induction of PML-ER for 1 or 2 days was not sufficient to induce a lasting senescence. However, induction of PML-ER with OHT for more than 3 days led to a stable senescent phenotype (Supplementary Fig. S6B). In contrast to normal cells, activation of PML-ER with OHT in PC3 prostate cancer cells only slightly reduced growth. Pretreatment of the cells, 6 days prior to the growth assay but not during the assay, with palbociclib or 5-Aza-dC alone moderately reduced cell growth in a dose-dependent manner (Fig. 6A and Supplementary Fig. S6C and S6D). However, inducing PML activation with OHT in tumor cells that were previously exposed to palbociclib or 5-Aza-dC lead to stronger growth arrest in response to both drugs (Fig. 6A and Supplementary Fig. S6C and S6D). These results suggest that the effects of 5-Aza-dC or palbociclib leading to cooperation with PML to induce senescence were imprinted in the cell population because they remained after the drugs were removed. In addition, most cells exposed sequentially to palbociclib or 5-Aza-dC and PML activation were unable to proliferate even after removal of the PML-ER inducer OHT (Fig. 6B and Supplementary Fig. S6E and S6F). Interestingly, pretreatment with palbociclib dramatically increased the growth arrest response to the chemotherapeutic drug camptothecin (Fig. 6C), indicating that its epigenetic effects facilitate the cellular senescence response to different agents.

Published OnlineFirst March 29, 2016; DOI: 10.1158/0008-5472.CAN-15-2347

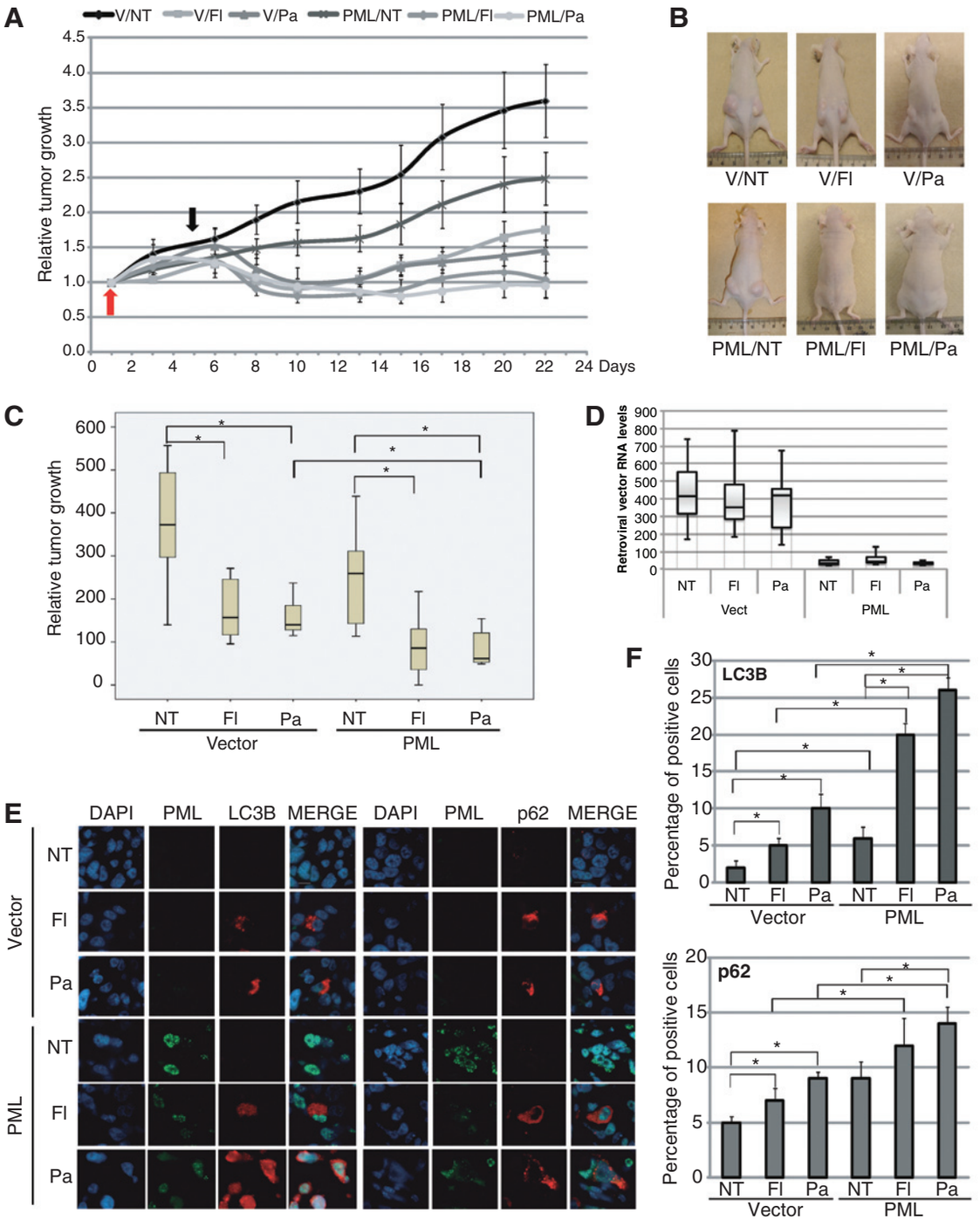

Figure 3.
CDK inhibitors enhance PML-mediated growth arrest and senescence in xenografts. A, relative tumor growth of PC3 cells expressing a vector control or PML injected subcutaneously in nude mice. Red arrow, the time at which tumors were approximately 150 mm^3 and treatment with flavopiridol (Fl; 5 mg/kg/d for 5 days) or palbociclib (Pa; 100 mg/kg/d for 5 days) started, $n = 8$/condition. Black arrow, the end of the five-day treatment. Each data point includes the SEM. B, representative pictures of tumors in the flanks of nude mice 22 days after the start of the treatments. C, box plot for the quantitation of tumor volume at day 22 in tumors as in A, *, $P < 0.05$ using Kruskal–Wallis test. D, box plot of qRT-PCR for the expression of the retroviral vector used to prepare PC3 vector control and PC3-PML cell populations using RNA extracted from tumors as in A. E, fluorescent imaging of LC3B and p62 as markers of autophagy vesicles (red) in tumors as in A. PML expression was visualized by indirect immunofluorescence (green); nuclei were visualized by DAPI staining (blue). Scale bar, 10 μm. F, quantification of cells positive for autophagic markers LC3B and p62 in tumors stained as in E. Three sets of 100 cells each were looked at, *, $P < 0.05$ using Student t test.

Published OnlineFirst March 29, 2016; DOI: 10.1158/0008-5472.CAN-15-2347

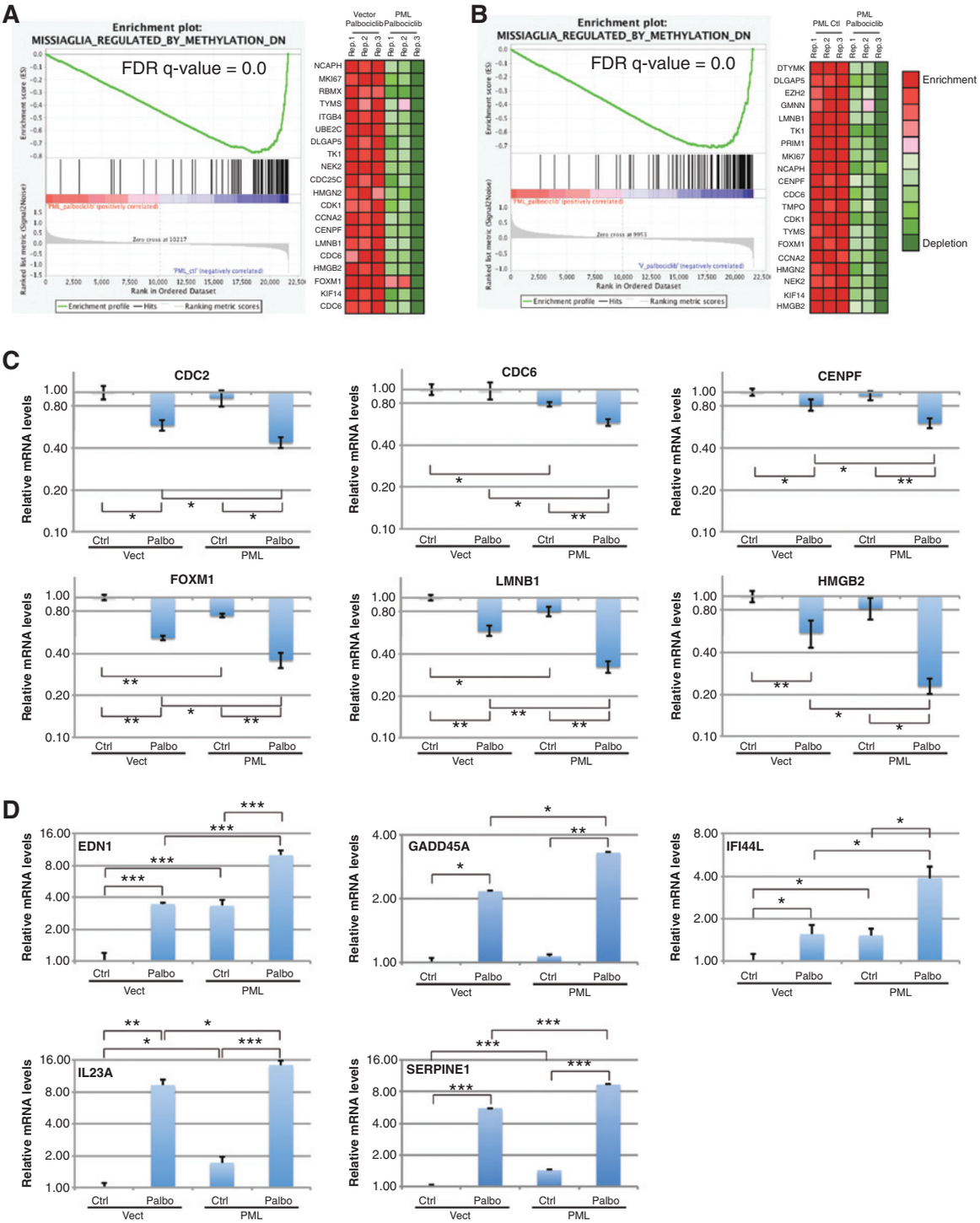

Figure 4.

Transcriptome analysis reveals methylation-sensitive genes as targets of PML and CDK-inhibitors. A and B, GSEA of microarray data comparing PC3 cells expressing PML and treated with palbociclib, with PC3 cells expressing PML but not treated (A) or with PC3 cells with an empty vector and treated with palbociclib (B). The gene set MISSIAGLIA_REGULATED_BY_METHYLATION_DN overlapped with genes altered in PC3 cells expressing PML and treated with palbociclib. The top 20 genes whose expression was most reduced in PML-expressing and palbociclib (Palbo)-treated PC3 cells are shown in heatmaps for each comparison. C, qPCR of selective genes downregulated by the combination of PML and palbociclib in PC3 cells overlapping with those downregulated by DNA methylation inhibitors in pancreatic cancer from the gene set MISSIAGLIA_REGULATED_BY_METHYLATION_DN. *, $P < 0.05$; **, $P < 0.01$; and ***, $P < 0.005$ using Student *t* test. D, qPCR of selected senescence regulatory genes normally repressed by DNA methylation and showing reexpression by the combination of PML and palbociclib in PC3 cells.

Published OnlineFirst March 29, 2016; DOI: 10.1158/0008-5472.CAN-15-2347

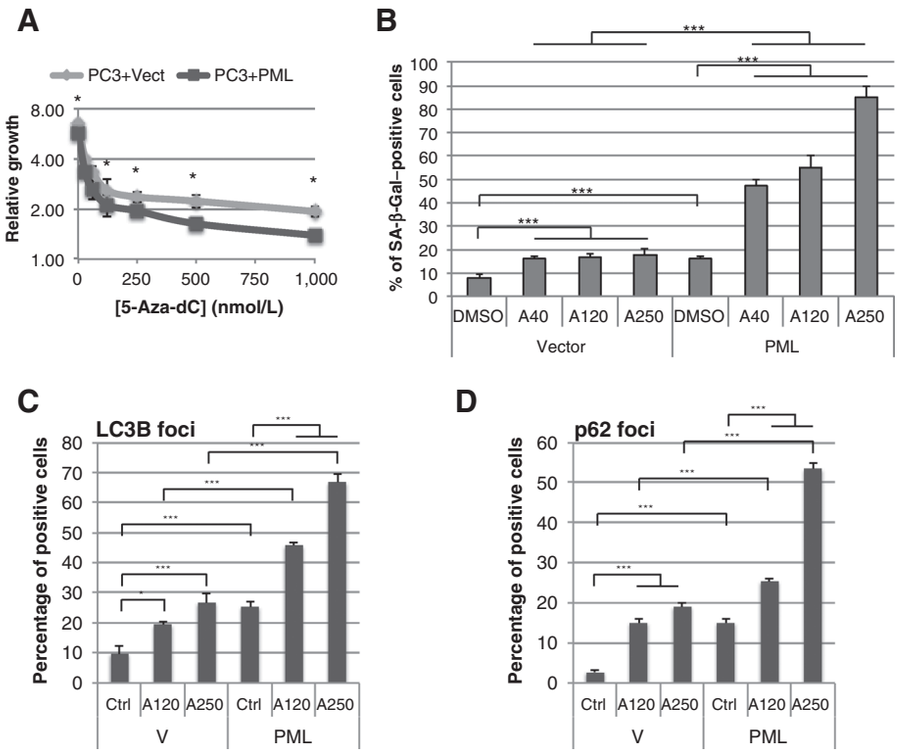

Figure 5.
A DNA methylation inhibitor enhances PML-mediated growth arrest and senescence in tumor cell lines. A, relative growth of PC3 cells infected with empty vector (Vect) or a vector expressing PML and treated with 5-Aza-dC at the indicated concentrations. Error bars, mean ± SD *, $P < 0.05$. B, SA-β-Gal in PC3 cells expressing either PML or a vector control and treated with 5-Aza-dC (A40, 40 nmol/L; A120, 120 nmol/L; A250, 250 nmol/L) or vehicle (DMSO). C and D, quantification of autophagy vesicles LC3B (C) and p62 (D) foci per cells after indirect immunofluorescence staining using specific antibodies. PC3 cells with an empty vector (V) or PML were treated with 5-Aza-dC at the indicated concentrations (A120, 120 nmol/L; A250, 250 nmol/L).

As the cooperation between PML and palbociclib led to changes in gene expression related to inhibition of DNA methylation and the DNMT1 inhibitor 5-Aza-dC has effects on tumor cells similar to palbociclib, we next explored whether palbociclib affected DNMT1 levels. We found that palbociclib decreased DNMT1 levels in a dose-dependent manner (Fig. 7A and Supplementary Fig. S7A). Of note, it has been reported that CDK1 and CDK2 phosphorylate DNMT1 at serine 154 stabilizing the protein (35). Using a phosphospecific antibody for this modification, we found that the levels of DNMT1 phosphorylated at serine 154 correlated with the levels of the total DNMT1 (Fig. 7A). Most likely, the reduced signal with the phosphospecific antibody is due to a corresponding reduction of the total levels of DNMT1. We next confirmed that reduction of CDK4 and CDK6 with shRNAs also reduced DNMT1 levels (Fig. 7B), suggesting that the effect of palbociclib is due to inhibition of these kinases and not an off target effect of the compound. Conversely, overexpression of CDK4 or CDK6 but not CDK2 dramatically increased DNMT1 levels in normal human fibroblasts (Fig. 7C). This effect of CDK4 or CDK6 on DNMT1 was not observed at the mRNA level (Fig. 7D), indicating an effect on translation or protein stability. The proteasome inhibitor MG132 was not able to rescue the levels of DNMT1 in palbociclib-treated cells (Fig. 7E). In contrast, the autophagy inhibitor bafilomycin A1 stabilized DNMT1 in palbociclib-treated cells (Fig. 7F). Taken together, these results are consistent with a model where CDK4 and CDK6 protect DNMT1 from autophagy-dependent protein degradation.

To investigate whether CDK4 can directly regulate DNMT1, we immunoprecipitated a flag-tagged allele of CDK4 expressed in HEK-293T cells with a Myc-tagged allele of DNMT1. We found DNMT1, after immunoblotting the CDK4 immunoprecipitates (Fig. 7G), suggesting a protein–protein interaction. Next, we used purified CDK4/cyclin D to assay for kinase activity on purified GST-DNMT1. We observed that CDK4/cyclin D phosphorylated DNMT1 *in vitro* (Fig. 7H). Finally, we used gel-purified GST-DNMT1 previously incubated with CDK4/cyclin D under kinase assay conditions to analyze the phosphorylation sites using mass spectrometry. We found that CDK4/cyclin D phosphorylated DNMT1 at serines 127 and 954 (Fig. 7I and Supplementary Fig. S7B). It has been reported that AKT can phosphorylate DNMT1 at serine 127 (36); however, this site fits better the consensus of a proline-directed kinase such as the CDKs. We found a single peptide phosphorylated at serine 247 but as this site does not fit the consensus of a proline-directed kinase we think it is not a relevant CDK4 phosphorylation site. Phosphorylation of DNMT1 at serine 954 has never been reported, but the site is close to a cluster of acetylation sites controlled by SirT1 (37), suggesting that these two modifications may functionally interact. Together, the results support a model where CDK4/6 regulate DNMT1 stability via its phosphorylation although it is also possible that these kinases may affect the autophagy program as well.

Discussion

Cellular senescence is a very efficient mechanism to prevent tumorigenesis that is triggered in normal cells after activation of oncogenes or a mitotic stress leading to telomere shortening (10). We show here that human cancer cells are resistant to PML-induced senescence due to hyperactive CDK4/6 signaling and that decreasing the activity of these kinases can restore the senescence response to PML activation. We found that CDK4/6 kinases control the phosphorylation and stability of DNMT1, which is required to maintain an epigenetic mechanism that prevents PML- and chemotherapy-induced senescence.

Published OnlineFirst March 29, 2016; DOI: 10.1158/0008-5472.CAN-15-2347

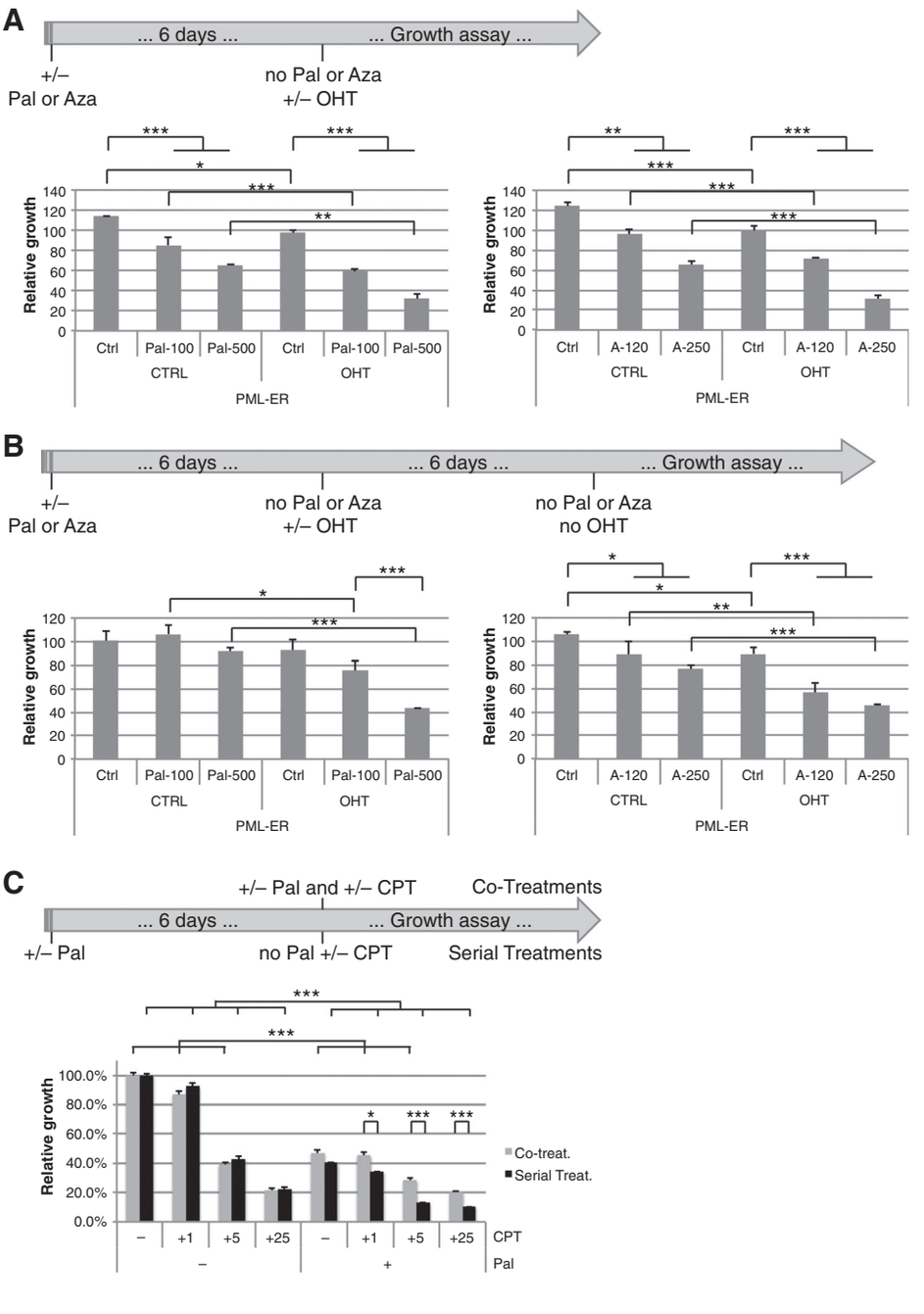

Figure 6.
Palbociclib or 5-Aza-dC confers sensitivity to PML- or camptothecin-induced permanent growth arrest. A, experimental timeline: PC3 cells expressing a PML-ER fusion are first treated with palbociclib [Pal-100 (100 nmol/L) or Pal-500 (500 nmol/L), every 3 days for 6 days] or 5-Aza-dC [A-120 (120 nmol/L) or A-250 (250 nmol/L), once over 3 days and then kept in normal medium for another 3 days]. Cells are then treated with ethanol 0.1% (CTRL, control) or 4-hydroxytamoxifen (OHT, 100 nmol/L) every 3 days over the next 6 days without further palbociclib (left graph) or 5-Aza-dC (right graph). Growth was estimated by a crystal violet retention assay. Results are shown as relative growth compared with cells expressing ER with only control treatments (see Supplementary Fig. S6C and S6D for full data set). B, as in A but the initial palbociclib or 5-Aza-dC temporary treatment is followed by a temporary treatment with control (CTRL, ethanol 0.1%) or 4-hydroxytamoxifen (OHT, 100 nmol/L) every 3 days over the next 6 days prior to plating for growth assay without any further treatment. Cells where fixed in glutaraldehyde and crystal violet retention was quantified. Results are shown as relative growth compared with cells expressing ER with only control treatments (see Supplementary Fig. S6E and S6F for full dataset). C, growth assay of cotreatments or serial treatments of PC3 cells with palbociclib and/or camptothecin. Cotreatments: PC3 cells were treated with vehicle control or 500 nmol/L palbociclib (+ Pal) along with control or various doses of camptothecin (+1: 1 nmol/L, +5: 5 nmol/L, +25: 25 nmol/L) every 3 days for 6 days. Serial treatments: PC3 cells were first treated with vehicle control (−) or 500 nmol/L palbociclib (+ Pal) every 3 days for 6 days and then treated with vehicle control or various doses of camptothecin (+1: 1 nmol/L, +5: 5 nmol/L, +25: 25 nmol/L) without further palbociclib. Growth was estimated by a crystal violet retention assay. (Student *t* test *P* values as follow: *, $P < 0.05$; **, $P < 0.01$; ***, $P < 0.005$).

The epigenetic marks maintained by DNMT1 in tumor cells to prevent senescence can act by several mechanisms including repression of prosenescence antiproliferative genes, enhancement of gene repression by RB–E2F complexes, and the control of genome stability. Our data supports these three nonexclusive possibilities. First, we identified several candidate tumor suppressors reexpressed in PC3 prostate cancer cells expressing PML and treated with the CDK4/6 inhibitor palbociclib. These genes were previously shown to be controlled by DNA methylation and include SerpinE1 (5, 38), IL23A (34), GKN2 (39), IGFBP3 (40), TNFAIP3 (41), IFI44L (33), SSX (42), EDN1 (31), and GADD45A (43). Consistent with this idea, it has been reported that DNA methylation inhibitors promote the expression of interferon target genes (30), many of which are known to play a role in senescence (44). Second, several E2F target genes were better repressed by the combination of PML and palbociclib (Fig. 5C), suggesting that inhibition of DNA methylation can enhance E2F targets gene repression by RB. In support of this mechanism, it has been reported that DNA binding by E2F transcription factors is sensitive to DNA methylation (45). Third, we found increased

Published OnlineFirst March 29, 2016; DOI: 10.1158/0008-5472.CAN-15-2347

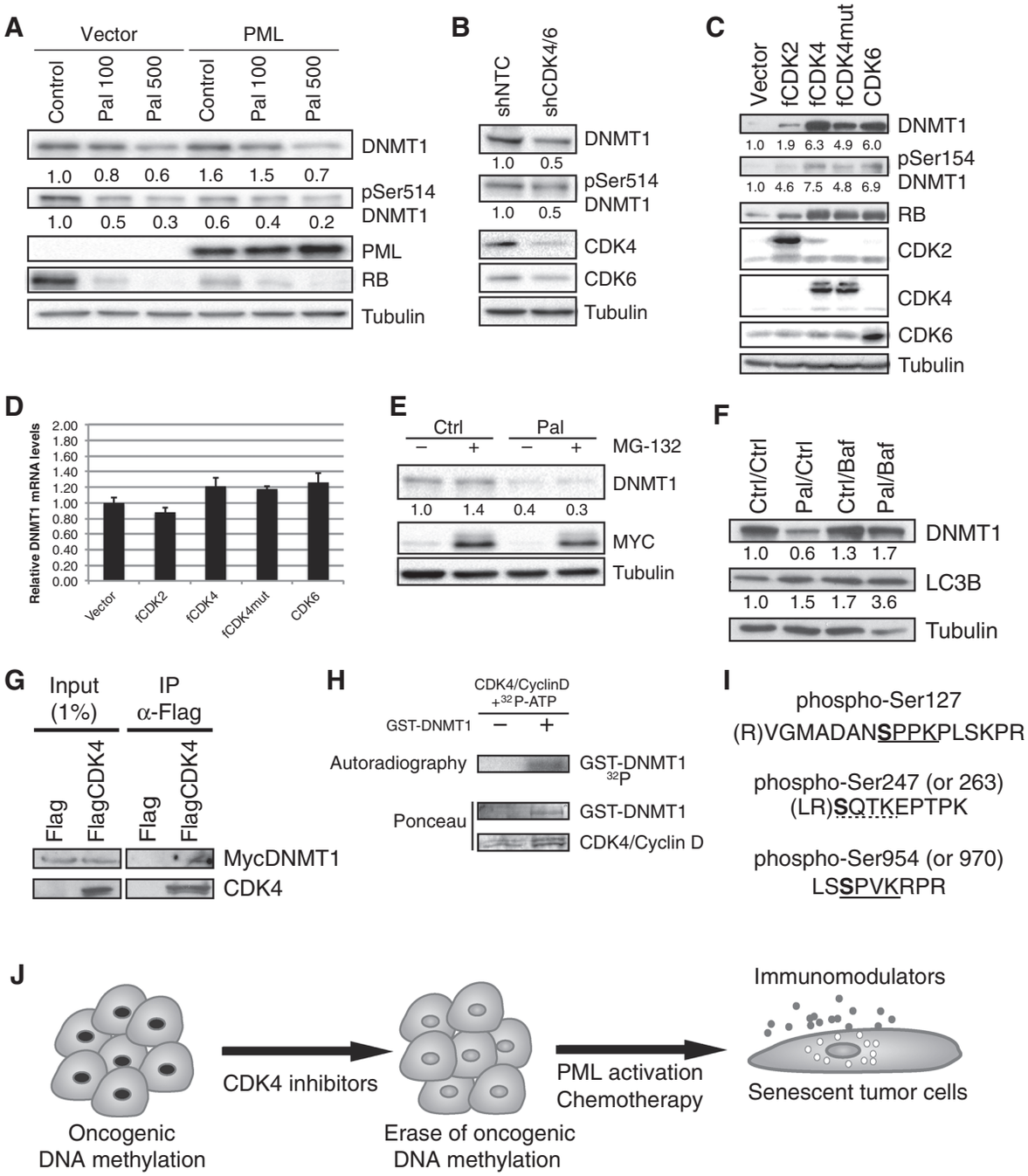

Figure 7.

CDK4 and CDK6 phosphorylate DNMT1, protecting it from autophagy-mediated degradation. A, immunoblots for the indicated proteins using extracts of PC3 cells expressing or not PML and treated or not over 6 days with CDK inhibitors palbociclib (Pal-100, 100 nmol/L; Pal-500, 500 nmol/L). B, immunoblots for the indicated proteins using PC3 cells infected with a control nontargeting shRNA (shNTC) or double shRNAs against CDK4 and CDK6 (shCDK4/6). C, immunoblots for the indicated proteins using extracts of IMR90 normal human fibroblast stably expressing a control vector, a flag-CDK2 (fCDK2), a flag-CDK4 (fCDK4), a flag-CDK4 mutant in K35M (fCDK4mut), or CDK6. D, qPCR of DNMT1 mRNA in cells as in C. E, immunoblots for the indicated proteins of PC3 cells treated with control vehicle (Ctrl) or with palbociclib (500 nmol/L; Pal) and treated with control (−) or proteasome inhibitor MG-132 (10 μmol/L) for 16 hours. Myc stabilization proves proteasome inhibition. F, immunoblots for the indicated proteins using extracts of PC3 cells treated for 24 hours with control vehicle (Ctrl) or palbociclib (500 nmol/L) and treated for 3 hours with control (Ctrl) or an autophagy inhibitor bafilomycin A1 (50 nmol/L). G, immunoblot for Myc-tag and CDK4 of an anti-flag coimmunoprecipitation experiment of HEK293T cell extracts expressing a vector flag or flag-CDK4 along with MycDNMT1. H, autoradiography for ^{32}P incorporation and Ponceau red staining of an *in vitro* kinase assay with purified CDK4/cyclin D and ^{32}P-ATP with or without purified GST-DNMT1. I, peptide sequences identified by mass spectrometry from gel purified GST-DNMT1 after *in vitro* kinase assay as in H, but with cold ATP. Phospho-serine 127 was identified in all 43 peptides sequenced. Phospho-serine 954 was identified in all eight peptides sequenced. Phospho-serine 247 was identified in one of six detected peptides. J, model for CDK4/6 inhibitors sensitizing cells to senescence as revealed in our study.

DNA damage signals in cells treated with palbociclib and PML, a phenomenon that can be explained by the role of DNMT1 controlling genome stability via methylation of juxtacentromeric satellite DNA (46).

The idea that DNA methylation prevents senescence is consistent with the widespread DNA hypomethylation observed in senescence cells using large-scale DNA methylation analysis (47). Hypomethylation in cells approaching senescence was linked to mislocalization of DNMT1 (47), indicating that DNMT1 is a key target to reprogram the genome for senescence. We add here a new mechanism controlling DNMT1 in senescence: decreased stability due to lack of CDK4/6-dependent phosphorylation of DNMT1. *In vitro*, CDK4 was able to phosphorylate DNMT1 at serines 127, 243, and 954 but further work will be required to precisely determine the role of each of these phosphorylation sites *in vivo*. Nevertheless, inhibition of CDK4/6 activity allowed autophagy-dependent degradation of DNMT1. Autophagy plays an important role in senescence controlling the expression of inflammatory cytokines (13, 14) and the nuclear envelope protein lamin B1 (48). We thus identified DNMT1 as a novel nuclear target of autophagy-dependent protein degradation in senescent cells. It is intriguing that lamin B1 and DNMT1 are targets for autophagy-dependent protein degradation and both control large-scale patterns of gene expression, suggesting that autophagy is mechanistically linked to genome reprogramming during cellular senescence.

It is still not clear how tumor cells acquire DNA methylation changes that block cellular senescence. DNMT1 is the most abundant DNA methyltransferase in cells and maintains DNA methylation patterns initially laid out by the *de novo* methylases DNMT3A and DNMT3B (49). An abnormal and cancer-specific gain of DNA methylation at promoters of tumor suppressor genes would require a mechanism to recruit *de novo* methylases to these promoters. Alternative, DNA methylation of tumor suppressors mediating senescence can be part of a normal mechanism that ensures self-renewal in stem cells and that requires DNMT1 for its maintenance. Consistent with this idea, DNMT1 is normally required to maintain populations of progenitor cells and prevent their exhaustion by cell differentiation (50). Reactivation of this program in tumor cells can explain why they acquire antisenescence epigenetic marks and drugs that can revert it should be promising for cancer therapeutics.

CDK4/6 inhibitors were conceived as cell-cycle inhibitors and are in clinical trials for the treatment of breast cancer and other malignancies (51). Our results linking this drug family to the control of epigenetic programs is unexpected and may justify their use beyond cell-cycle control. It is plausible that in addition to their cell-cycle effects their clinical efficacy is related to their ability to inactivate DNMT1 and sensitize cells for irreversible senescent cell-cycle arrest (Fig. 7J). Our results showing cooperation between CDK4/6 inhibitors and the senescence regulator PML may also indicate that PML status in tumors can predict the response to these drugs. It has been recognized that chemotherapeutic agents can induce tumor cell senescence (11) and CDK4/6 inhibitors can enhance this response acting as erasers of tumor epigenetic marks. Likely, these drugs could be widely used to improve the effect of a variety of chemotherapeutic agents.

Disclosure of Potential Conflicts of Interest

No potential conflicts of interest were disclosed.

Authors' Contributions

Conception and design: M. Acevedo, M. Vernier, V. Bourdeau, G. Ferbeyre
Development of methodology: M. Acevedo, M. Vernier, O. Moiseeva, V. Bourdeau, G. Ferbeyre
Acquisition of data (provided animals, acquired and managed patients, provided facilities, etc.): M. Acevedo, M. Vernier, L. Mignacca
Analysis and interpretation of data (e.g., statistical analysis, biostatistics, computational analysis): M. Acevedo, G. Huot, V. Bourdeau, G. Ferbeyre
Writing, review, and/or revision of the manuscript: M. Acevedo, M. Vernier, V. Bourdeau, G. Ferbeyre
Administrative, technical, or material support (i.e., reporting or organizing data, constructing databases): G. Huot, V. Bourdeau
Study supervision: V. Bourdeau, G. Ferbeyre
Other (performed the experiments shown in Fig. 7G–I.): F. Lessard

Acknowledgments

The authors thank the Center for Advanced Proteomics Analyses at the Université de Montréal/Institute for Research in Immunology and Cancer for the mass spectrometry analysis. The authors also thank S. Lowe for reagents and F. Badeaux and V. Limoges for cloning of pBABE-PML-ER.

Grant Support

This work was funded by grant CIHR RN196161-300726.

The costs of publication of this article were defrayed in part by the payment of page charges. This article must therefore be hereby marked *advertisement* in accordance with 18 U.S.C. Section 1734 solely to indicate this fact.

Received August 26, 2015; revised February 10, 2016; accepted March 10, 2016; published OnlineFirst March 29, 2016.

References

1. Ferbeyre G. PML a target of translocations in APL is a regulator of cellular senescence. Leukemia 2002;16:1918–26.
2. Ferbeyre G, de Stanchina E, Querido E, Baptiste N, Prives C, Lowe SW. PML is induced by oncogenic ras and promotes premature senescence. Genes Dev 2000;14:2015–27.
3. Pearson M, Carbone R, Sebastiani C, Cioce M, Fagioli M, Saito S, et al. PML regulates p53 acetylation and premature senescence induced by oncogenic Ras. Nature 2000;406:207–10.
4. Bischof O, Kirsh O, Pearson M, Itahana K, Pelicci PG, Dejean A. Deconstructing PML-induced premature senescence. EMBO J 2002;21:3358–69.
5. Ablain J, Rice K, Soilihi H, de Reynies A, Minucci S, de The H. Activation of a promyelocytic leukemia-tumor protein 53 axis underlies acute promyelocytic leukemia cure. Nat Med 2014;20:167–74.
6. Trotman LC, Alimonti A, Scaglioni PP, Koutcher JA, Cordon-Cardo C, Pandolfi PP. Identification of a tumour suppressor network opposing nuclear Akt function. Nature 2006;441:523–7.
7. Mallette FA, Goumard S, Gaumont-Leclerc MF, Moiseeva O, Ferbeyre G. Human fibroblasts require the Rb family of tumor suppressors, but not p53, for PML-induced senescence. Oncogene 2004;23:91–9.
8. Vernier M, Bourdeau V, Gaumont-Leclerc MF, Moiseeva O, Begin V, Saad F, et al. Regulation of E2Fs and senescence by PML nuclear bodies. Genes Dev 2011;25:41–50.
9. Bischof O, Nacerddine K, Dejean A. Human papillomavirus oncoprotein E7 targets the promyelocytic leukemia protein and circumvents cellular senescence via the Rb and p53 tumor suppressor pathways. Mol Cell Biol 2005;25:1013–24.

Published OnlineFirst March 29, 2016; DOI: 10.1158/0008-5472.CAN-15-2347

10. Burton DG, Krizhanovsky V. Physiological and pathological consequences of cellular senescence. Cell Mol Life Sci 2014;71:4373–86.
11. Schmitt CA. Senescence, apoptosis and therapy–cutting the lifelines of cancer. Nat Rev Cancer 2003;3:286–95.
12. Lee BY, Han JA, Im JS, Morrone A, Johung K, Goodwin EC, et al. Senescence-associated beta-galactosidase is lysosomal beta-galactosidase. Aging Cell 2006;5:187–95.
13. Young AR, Narita M, Ferreira M, Kirschner K, Sadaie M, Darot JF, et al. Autophagy mediates the mitotic senescence transition. Genes Dev 2009;23:798–803.
14. Kang C, Xu Q, Martin TD, Li MZ, Demaria M, Aron L, et al. The DNA damage response induces inflammation and senescence by inhibiting autophagy of GATA4. Science 2015;349:aaa5612.
15. Sherman MY, Meng L, Stampfer M, Gabai VL, Yaglom JA. Oncogenes induce senescence with incomplete growth arrest and suppress the DNA damage response in immortalized cells. Aging Cell 2011;10:949–61.
16. Michaloglou C, Vredeveld LC, Soengas MS, Denoyelle C, Kuilman T, van der Horst CM, et al. BRAFE600-associated senescence-like cell cycle arrest of human naevi. Nature 2005;436:720–4.
17. Talluri S, Dick FA. The retinoblastoma protein and PML collaborate to organize heterochromatin and silence E2F-responsive genes during senescence. Cell Cycle 2014;13:641–51.
18. Chicas A, Wang X, Zhang C, McCurrach M, Zhao Z, Mert O, et al. Dissecting the unique role of the retinoblastoma tumor suppressor during cellular senescence. Cancer Cell 2010;17:376–87.
19. Vernier M, Ferbeyre G. Complete senescence: RB and PML share the task. Cell Cycle 2014;13:696.
20. Narita M, Nunez S, Heard E, Lin AW, Hearn SA, Spector DL, et al. Rb-mediated heterochromatin formation and silencing of E2F target genes during cellular senescence. Cell 2003;113:703–16.
21. Narita M, Narita M, Krizhanovsky V, Nunez S, Chicas A, Hearn SA, et al. A novel role for high-mobility group a proteins in cellular senescence and heterochromatin formation. Cell 2006;126:503–14.
22. Braig M, Lee S, Loddenkemper C, Rudolph C, Peters AH, Schlegelberger B, et al. Oncogene-induced senescence as an initial barrier in lymphoma development. Nature 2005;436:660–5.
23. Di Micco R, Sulli G, Dobreva M, Liontos M, Botrugno OA, Gargiulo G, et al. Interplay between oncogene-induced DNA damage response and heterochromatin in senescence and cancer. Nat Cell Biol 2011;13:292–302.
24. Deschenes-Simard X, Gaumont-Leclerc MF, Bourdeau V, Lessard F, Moiseeva O, Forest V, et al. Tumor suppressor activity of the ERK/MAPK pathway by promoting selective protein degradation. Genes Dev 2013;27:900–15.
25. Subramanian A, Tamayo P, Mootha VK, Mukherjee S, Ebert BL, Gillette MA, et al. Gene set enrichment analysis: a knowledge-based approach for interpreting genome-wide expression profiles. Proc Natl Acad Sci U S A 2005;102:15545–50.
26. Moiseeva O, Deschenes-Simard X, St-Germain E, Igelmann S, Huot G, Cadar AE, et al. Metformin inhibits the senescence-associated secretory phenotype by interfering with IKK/NF-kappaB activation. Aging Cell 2013;12:489–98.
27. Chao SH, Price DH. Flavopiridol inactivates P-TEFb and blocks most RNA polymerase II transcription in vivo. J Biol Chem 2001;276:31793–9.
28. Fry DW, Harvey PJ, Keller PR, Elliott WL, Meade M, Trachet E, et al. Specific inhibition of cyclin-dependent kinase 4/6 by PD 0332991 and associated antitumor activity in human tumor xenografts. Mol Cancer Ther 2004;3:1427–38.
29. Coppe JP, Patil CK, Rodier F, Sun Y, Munoz DP, Goldstein J, et al. Senescence-associated secretory phenotypes reveal cell-nonautonomous functions of oncogenic RAS and the p53 tumor suppressor. PLoS Biol 2008;6:2853–68.
30. Missiaglia E, Donadelli M, Palmieri M, Crnogorac-Jurcevic T, Scarpa A, Lemoine NR. Growth delay of human pancreatic cancer cells by methylase inhibitor 5-aza-2′-deoxycytidine treatment is associated with activation of the interferon signalling pathway. Oncogene 2005;24:199–211.
31. Wiesmann F, Veeck J, Galm O, Hartmann A, Esteller M, Knuchel R, et al. Frequent loss of endothelin-3 (EDN3) expression due to epigenetic inactivation in human breast cancer. Breast Cancer Res 2009;11:R34.
32. Bulavin DV, Kovalsky O, Hollander MC, Fornace AJJr. Loss of oncogenic H-ras-induced cell cycle arrest and p38 mitogen-activated protein kinase activation by disruption of Gadd45a. Mol Cell Biol 2003;23:3859–71.
33. Coit P, Jeffries M, Altorok N, Dozmorov MG, Koelsch KA, Wren JD, et al. Genome-wide DNA methylation study suggests epigenetic accessibility and transcriptional poising of interferon-regulated genes in naive CD4+ T cells from lupus patients. J Autoimmun 2013;43:78–84.
34. Lin Z, Hegarty JP, Yu W, Cappel JA, Chen X, Faber PW, et al. Identification of disease-associated DNA methylation in B cells from Crohn's disease and ulcerative colitis patients. Dig Dis Sci 2012;57:3145–53.
35. Lavoie G, St-Pierre Y. Phosphorylation of human DNMT1: implication of cyclin-dependent kinases. Biochem Biophys Res Commun 2011;409:187–92.
36. Hervouet E, Lalier L, Debien E, Cheray M, Geairon A, Rogniaux H, et al. Disruption of Dnmt1/PCNA/UHRF1 interactions promotes tumorigenesis from human and mice glial cells. PLoS One 2010;5:e11333.
37. Peng L, Yuan Z, Ling H, Fukasawa K, Robertson K, Olashaw N, et al. SIRT1 deacetylates the DNA methyltransferase 1 (DNMT1) protein and alters its activities. Mol Cell Biol 2011;31:4720–34.
38. Patel N, Black J, Chen X, Marcondes AM, Grady WM, Lawlor ER, et al. DNA methylation and gene expression profiling of ewing sarcoma primary tumors reveal genes that are potential targets of epigenetic inactivation. Sarcoma 2012;2012:498472.
39. Lu F, Tempera I, Lee HT, Dewispelaere K, Lieberman PM. EBNA1 binding and epigenetic regulation of gastrokine tumor suppressor genes in gastric carcinoma cells. Virol J 2014;11:12.
40. Tomii K, Tsukuda K, Toyooka S, Dote H, Hanafusa T, Asano H, et al. Aberrant promoter methylation of insulin-like growth factor binding protein-3 gene in human cancers. Int J Cancer 2007;120:566–73.
41. Chanudet E, Huang Y, Ichimura K, Dong G, Hamoudi RA, Radford J, et al. A20 is targeted by promoter methylation, deletion and inactivating mutation in MALT lymphoma. Leukemia 2010;24:483–7.
42. Dubovsky JA, McNeel DG. Inducible expression of a prostate cancer-testis antigen, SSX-2, following treatment with a DNA methylation inhibitor. Prostate 2007;67:1781–90.
43. Wang W, Huper G, Guo Y, Murphy SK, Olson JAJr., Marks JR. Analysis of methylation-sensitive transcriptome identifies GADD45a as a frequently methylated gene in breast cancer. Oncogene 2005;24:2705–14.
44. Moiseeva O, Mallette FA, Mukhopadhyay UK, Moores A, Ferbeyre G. DNA Damage Signaling and p53-dependent Senescence after Prolonged beta-Interferon Stimulation. Mol Biol Cell 2006;17:1583–92.
45. Campanero MR, Armstrong MI, Flemington EK. CpG methylation as a mechanism for the regulation of E2F activity. Proc Natl Acad Sci U S A 2000;97:6481–6.
46. Rhee I, Jair KW, Yen RW, Lengauer C, Herman JG, Kinzler KW, et al. CpG methylation is maintained in human cancer cells lacking DNMT1. Nature 2000;404:1003–7.
47. Cruickshanks HA, McBryan T, Nelson DM, Vanderkraats ND, Shah PP, van Tuyn J, et al. Senescent cells harbour features of the cancer epigenome. Nat Cell Biol 2013;15:1495–506.
48. Dou Z, Xu C, Donahue G, Shimi T, Pan JA, Zhu J, et al. Autophagy mediates degradation of nuclear lamina. Nature 2015;527:105–9.
49. Jones PA, Liang G. Rethinking how DNA methylation patterns are maintained. Nat Rev 2009;10:805–11.
50. Sen GL, Reuter JA, Webster DE, Zhu L, Khavari PA. DNMT1 maintains progenitor function in self-renewing somatic tissue. Nature 2010;463:563–7.
51. Law ME, Corsino PE, Narayan S, Law BK. Cyclin-dependent kinase inhibitors as anticancer therapeutics. Mol Pharmacol 2015;88:846–52.

Published OnlineFirst March 29, 2016; DOI: 10.1158/0008-5472.CAN-15-2347

Cancer Research
The Journal of Cancer Research (1916–1930) | The American Journal of Cancer (1931–1940)

AACR American Association for Cancer Research

A CDK4/6-Dependent Epigenetic Mechanism Protects Cancer Cells from PML-induced Senescence

Mariana Acevedo, Mathieu Vernier, Lian Mignacca, et al.

Cancer Res 2016;76:3252-3264. Published OnlineFirst March 29, 2016.